Supplementary S1. Sample design and fabrication

The photonic crystals (PCs) were designed to enable the excitation of the optical surface mode in the vicinity of the total internal reflection angle for the glass-air interface. The parameters of the PCs were selected to achieve close to the quarter-wavelength layer thickness, and thus, to have the centre of the PC bandgap at the corresponding total internal reflection angle and incident light wavelength. At the same time, the layer widths were tuned to minimize the integral thickness of the PCs[42]. This is important, since for the p-polarization one needs to deposit more than 10 pairs of layers in order to achieve suitable Bragg reflectance in the bandgap at oblique incidence.

The PCs were deposited on a fused silica substrate using magnetron sputtering and comprised dielectric non-magnetic tantalum pentoxide (Ta_2O_5, 119.3 nm) and silicon oxide (SiO_2, 164.4 nm) layers. The PC for the BIG+Pt sample had 16 pairs of layers; whereas the Py+Ta sample PC had 14 pairs of layers with the additional Ta_2O_5 layer of 107.5 nm width. A layer of bismuth-substituted iron garnet ($Bi_{2.1}Dy_{0.9}Fe_{3.9}Ga_{1.1}O_{12}$, 125 nm) was deposited on top of the PC for the BIG+Pt sample. After that, the PC with iron-garnet was annealed at 600°C to transform it to ferromagnetic, and this process slightly changes its permittivity. Thin layers of Pt, Py and Ta were deposited via magnetron sputtering.

Supplementary S2. Experimental setup and data processing

Measurements were performed at room temperature. For the excitation of the surface plasmonic resonance in a thin metal film of the magnetoplasmonic heterostructure we used the Kretschmann configuration. The sample was fixed on a SiO_2 prism having a base angle of 42° (which is close to the angle of total internal reflection) using an index matching oil.

The structure was illuminated by a laser diode of wavelength of 805 nm and power 50 mW. The p-polarization of the laser beam was adjusted with a polarizer, and then the beam was modulated with an optical chopper operating at a frequency of 360 Hz. Modulated laser beam was focused on the sample via a micro-objective, the diameter of the focused beam was 100 μm. The angle of incidence was varied from 30 to 60 degrees through rotation of the holder on which the sample was fixed. The angular rotation accuracy was 0.05°.

The reflected light was detected by a photodiode. The sample was placed in the in-plane external magnetic field H_{ext}=150mT created by the electromagnet along y-axis (fig.1a). The external magnetic field $\mathbf{H_{ext}}$ was modulated by a sinusoidal signal at a frequency of 1.5 kHz. The resulting optically induced voltage was measured via electrodes attached to the surface of the sample using conductive glue, and amplified by a differential voltage amplifier with a gain of 1000 and an input noise level of 1nV/Hz$^{0.5}$, and then digitized using a National Instruments USB-6351 data acquisition board. Then, the signal was Fourier transformed.

Chopper makes a square-wave modulation of the optical signal $I(t) = \frac{1}{2}I_0(1 + \sin\omega_{ch}t + \frac{1}{3}\sin 3\omega_{ch}t + \frac{1}{5}\sin 5\omega_{ch}t + \ldots) + I_\eta$ with I_η mimicking some noise-related offset. Similar square-wave temporal dependence stays for the sample magnetization modulation under the action of $H_{ext} > H_{sat}$: $M = M_0(\sin(\omega_H t + \phi) + \frac{1}{3}\sin(3\omega_H t + \phi) + \frac{1}{5}\sin(5\omega_H t + \phi) + \ldots) + M_\eta$, where ϕ is a phase shift between the optical and magnetic field modulation. As the generated due to the ISHE and ANE effects voltage is proportional to $V_{sum} \sim I \cdot M$, the measured voltage

$$V_{sum} \sim \frac{1}{4}I_0M_0\{2(1 + I_\eta)\sin(\omega_H t + \phi) + 2M_\eta sin\omega_{ch}t + \sin[(\omega_{ch} + \omega_H)t + \phi) + \sin[(\omega_{ch} - \omega_H)t - \phi] + \frac{1}{3}$$
$$\sin[(3\omega_{ch} - \omega_H)t - \phi) + \sin[(3\omega_{ch} + \omega_H)t + \phi) + \ldots\}$$

. Thus, due to the presence of two modulating frequencies, the frequency of the modulating external magnetic field and the optical chopper operation frequency, the resulting Fourier spectra of the signal have the corresponding sum and difference frequencies at which the amplitude of the induced voltage was measured. In the present setup, the magnitude of the $V_{(\omega_{ch} + \omega_H)} \sim V\sin[(\omega_{ch} + \omega_H)t - \phi]$ component was measured. It is directly proportional to the odd in magnetization modulation of the induced voltage. It is important that $V_{(\omega_{ch} + \omega_H)}$ signal is completely insensitive to any time-independent offsets and low-frequency noises since they contribute only to $m\omega_H$ and $m\omega_{ch}$ harmonics (m=1,3,5…).

Supplementary S3. Numerical simulation and structure optimization

The optical properties of the opto-spintronic structures were simulated using the impedance method proposed in [32] for layered structures. The method is based on analytical recursive calculation of the so-called optical impedances $Z = \frac{E_\tau}{H_\tau}$ of the structure using the Fresnel formulas, which allow near- and far- field characteristics of the structure, the reflectance, transmittance and absorption to be obtained analytically.

The PC-based structures were optimized to obtain the narrow and deep resonances corresponding to the surface mode excitation. However, one should bear in mind that the angular width of the laser beam must typically be focused in order to achieve higher intensity. This makes it difficult to benefit from the inherent ultra-narrow surface mode resonances. The key advantage of the proposed nanostructure is that one may tune not only the position, but also the width of the resonance. Assuming the resonance curves have Lorentzian shapes[57], then

$$R(k_x) = 1 - \frac{4\Gamma_i\Gamma_{rad}}{(\beta_{mode} - k_x)^2 + (\Gamma_i + \Gamma_{rad})^2}$$

One may observe that the resonance angular width is determined by the sum of Joule Γ_i and radiation Γ_{rad} losses, i.e., $\Gamma_i + \Gamma_{rad}$. However, in any structure it is possible to achieve deep resonance with $R_{min} \approx 0\%$ by tuning the structure to make $\Gamma_{rad} = \Gamma_i$, since Γ_{rad} is directly controlled by the number of layers in the PC structure.

The purple curve in Fig. 3a shows a nanostructure with wider surface optical mode resonance. The PC comprises 14 layers of 109 nm thick Ta_2O_5 and 181 nm thick SiO_2 covered with 120 nm of BIG and 1 nm of Pt. Tuning the thickness of the terminating layer results in a shift of the resonant wavelength by 1 nm per approximately 1nm change in the thickness of the considered PC.

Supplementary S4. PC parameters variation under annealing

PC covered with bismuth-substituted iron-garnet requires annealing at 600°C to transform BIG to the ferromagnetic phase. The red shift of the photonic crystal bandgap edges (~50 nm approximately) was observed during this process as shown in Fig.S4.1. This effect was treated as the variation of the layer's permittivity values (2-3%) probably due to the additional oxidation process. The numerical models were corrected to match the new measured spectra. At the operating wavelength of 805 nm ε_{BIG}=5.52+0.018i, $\varepsilon_{Ta2O5} = 4.6200 + 0.0016i$, $\varepsilon_{SiO2} = 2.1911 + 0.0007i$.

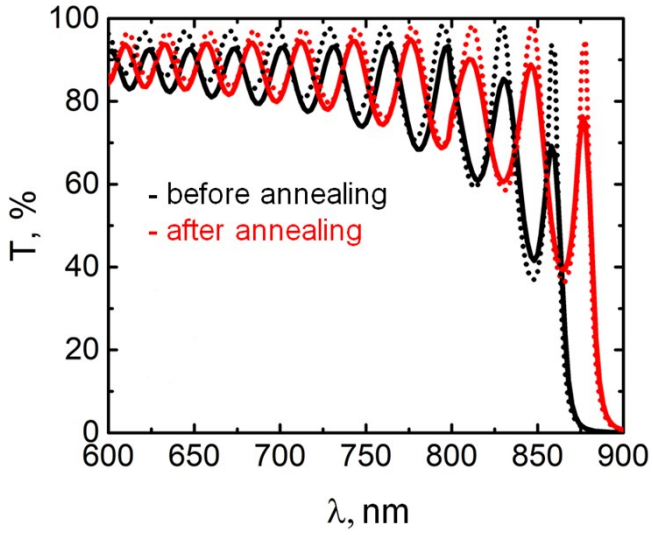

Figure S4.1 The transmittance spectra of the photonic crystal before (black color) and after (red color) annealing ($600^\circ C$, $10\ min$) measured (solid lines) and calculated (dotted lines) at normal incidence of light.